Radiology

# MR Imaging of Treated Prostate Cancer[1]

Hebert Alberto Vargas, MD
Cecilia Wassberg, MD, PhD
Oguz Akin, MD
Hedvig Hricak, MD, PhD, Dr(hc)

**Online CME**
*See www.rsna.org/ry_cme.html*

**Learning Objectives:**

- Discuss prostate cancer treatment strategies and the conventional MR imaging techniques used for assessment of the pelvic region after treatment for prostate cancer.

- Describe the clinical settings in which various MR techniques (MR spectroscopic, diffusion-weighted, and dynamic contrast-enhanced imaging) may be helpful.

- Recognize normal and abnormal MR imaging findings after treatment for prostate cancer.

Many management options are available to patients with newly diagnosed prostate cancer. Magnetic resonance (MR) imaging plays an important role in initial staging of prostate cancer, but it also aids in tumor detection when there is clinical or biochemical suspicion of residual or recurrent disease after treatment. The purpose of this review is to describe the normal appearances of the prostatic region after different kinds of treatment for prostate cancer and to discuss how these appearances differ from those of recurrent and residual disease. Several MR imaging techniques used in evaluating patients with prostate cancer are described, including conventional MR imaging sequences (mainly T1- and T2-weighted sequences), MR spectroscopic imaging, diffusion-weighted imaging, and dynamic contrast agent–enhanced MR imaging. Clinical considerations, together with the different approaches for interpreting serum prostate-specific antigen values in the posttreatment setting, are also presented. All forms of treatment alter the MR imaging features of the prostatic region to a greater or lesser extent, and it is important to be able to recognize expected posttreatment appearances and distinguish them from the features of recurrent or residual cancer to aid subsequent clinical management.

© RSNA, 2012

Radiology

## Essentials

- The most important role of imaging is to localize recurrence when it is suspected, so that observation (if no recurrence is detected), salvage therapy (in the presence of local recurrence), or systemic therapy (in the presence of widespread disease) can be promptly instituted.

- The most common site of local recurrence after radical prostatectomy is the vesicourethral anastomosis; the typical MR imaging appearance of recurrence is an enhancing soft-tissue nodule that is isointense to muscle on T1-weighted images and slightly hyperintense to muscle on T2-weighted images.

- The main effects of radiation therapy (RT) on the MR imaging appearance of the prostate are a decrease in size and diffusely decreased signal intensity on T2-weighted images due to glandular loss and fibrosis; recurrent tumor typically appears on T2-weighted images as a nodular lesion of lower signal intensity than the adjacent treated prostate, with restricted diffusion and rapid enhancement, in the same location as the pre-RT tumor.

- The imaging features of the treated prostate and of prostate cancer recurrence after androgen-deprivation therapy may be similar to those after RT (decreased volume, decreased signal intensity on T2-weighted images, loss of zonal differentiation); however, RT-induced changes in adjacent structures are absent; at MR imaging and MR spectroscopic imaging, patients demonstrate diverse morphologic and metabolic responses, with the magnitude of responses depending on the type and duration of therapy.

- After focal therapies, MR imaging is used to assess the extent and distribution of the expected necrosis in the target region: On contrast-enhanced T1-weighted images, nonenhancing low-signal-intensity regions are expected at sites of treated tumors (representing necrosis), while focal areas of enhancement (representing viable tissue) are suspicious for recurrence.

The prostate is the most common noncutaneous site of cancer in men. In the United States, approximately one in six men will develop prostate cancer at some point in life (1). Management options are numerous; a recent study of the primary treatment received by 11 892 men with newly diagnosed prostate cancer showed that approximately 7% elected active surveillance; 50%, radical prostatectomy; 12%, external-beam radiation therapy (RT); 13%, brachytherapy; 4%, cryoablation; and 14%, androgen-deprivation therapy (2). Other treatments such as high-intensity focused ultrasound and photodynamic therapy are also becoming increasingly available. Continuous improvements and refinements in these treatment strategies, together with a trend toward earlier detection and a decrease in prostate cancer stage at the time of diagnosis, have resulted in a 99% relative survival rate 5 years after initial diagnosis (1). However, a proportion of treated patients have prostate cancer recurrence, which is often first suspected on the basis of abnormal digital rectal examination findings or increasing serum prostate-specific antigen (PSA) levels. Magnetic resonance (MR) imaging can play an important role in the assessment of these patients. In this review, we will discuss the normal appearances of the prostate and prostatic bed after different kinds of treatment and how these appearances differ from those of recurrent and residual prostate cancer. Several MR imaging techniques used in evaluating patients with prostate cancer will be described, including conventional MR imaging, MR spectroscopic imaging, diffusion-weighted MR imaging, and dynamic contrast material–enhanced MR imaging.

### Overview of MR Imaging Techniques and Protocols

Prostate MR imaging can be performed with a 1.5- or 3-T whole-body unit. For optimal image quality, a body coil is used for excitation and a pelvic phased-array coil combined with an endorectal coil is used for signal reception. The standard protocol includes large-field-of-view (24–26 cm) transverse T1-weighted sequences, mainly to assess the pelvic bones, lymph nodes, and, if prostatic tissue remains, the presence of post-biopsy changes that may hinder the interpretation of images obtained with other sequences. Transverse, coronal, and sagittal T2-weighted sequences with a small field of view (12–14 cm) are also performed for detailed assessment of the prostatic fossa and seminal vesicles (3).

MR spectroscopic imaging allows detection of multiple metabolites (including citrate, choline, polyamines, and creatine) in tissues. Variations in the presence and concentration of such metabolites form the basis for differentiating cancerous from noncancerous tissues by using MR spectroscopic imaging. Typically, the citrate level is high in normal prostatic tissue, owing to the fact that the presence of zinc inhibits the first enzyme in the Krebs cycle (4,5). Citrate levels are reduced in prostate cancer, but they can also be decreased as a result of prostatitis or hemorrhage (6). Choline is a constituent of the cell membrane, and, as such, its levels increase with the increased membrane turnover and phospholipids metabolism seen in prostate cancer (7,8). The polyamine level peak occurs between the creatine and choline level peaks and is typically decreased in prostate cancer (9). Metabolite ratios, such as the choline-plus-creatine–to-citrate and choline-to-creatine ratios, can also be calculated, and these have been shown to be useful in differentiating benign from malignant tissue voxels (10). In practice, evaluation of the spectroscopic data can be performed quantitatively by using the numeric values of

these metabolic peaks and ratios, but qualitative assessment based on visual evaluation of the metabolite peaks can also be performed. This approach is particularly useful when there is overlapping noise or incorrect integration (11). The technique is commonly performed with point-resolved spatial selection, or PRESS, voxel excitation and band-selective inversion with gradient dephasing or spectral-spatial pulses for water and lipid suppression.

Diffusion-weighted (DW) MR imaging derives its image contrast from differences between the rates of water movement in different biologic tissues. Water motion, or *diffusion,* in malignant tumors is restricted relative to that in normal tissue (12). By obtaining multiple images with different diffusion weighting factors (*b* values), it is possible to calculate the apparent diffusion coefficient (ADC)—a measure of the area water molecules have traveled in a unit of time, usually reported as square millimeters per second. The ADCs are calculated for all pixels of the image and are displayed as a parametric map (ADC map). DW images are obtained in the axial plane by using a spin-echo echoplanar sequence with a pair of gradient pulses along one or more directions. Multiple *b* values are used, usually in the range of 0–1500 sec/mm².

The principle behind enhancement on dynamic contrast-enhanced MR images is the effect of an intravenously administered gadolinium-based contrast agent on relaxation rate in a tissue of interest. Malignant tumors tend to enhance earlier and more avidly than do surrounding tissues. In conventional contrast-enhanced imaging, data are acquired statically before and at two or three time points (eg, 1, 2, and 3 minutes) after contrast agent administration. Alternatively, with the dynamic approach, sequential images are acquired more rapidly during the passage of a contrast agent through a volume of interest so that signal intensity can be assessed as a function of time. The basis for the utility of this technique is that the characteristic angiogenesis in prostate cancer results in rapid

contrast agent uptake and washout, and this behavior can be better depicted by using a dynamic acquisition. A typical dynamic contrast-enhanced MR imaging acquisition involves a three-dimensional T1-weighted spoiled gradient-echo sequence with a temporal resolution of about 7–8 seconds to cover the entire prostate during 4–5 minutes after intravenous injection of 0.1 mmol gadolinium chelate per kilogram of body weight at a rate of 2 mL/sec. Contrast enhancement–time curves can be generated, and they will reflect the changes in MR signal intensity resulting from the passage of contrast agent through a given region of interest over time. Pharmacokinetic models are also used to characterize tissue permeability, which, in tumors, reflects perfusion because of high first-pass extraction fraction values. Several pharmacokinetic models have been proposed to characterize tissue perfusion on dynamic contrast-enhanced MR images. Often used is a bicompartmental model developed by Tofts et al (13) from which several variables can be quantitatively measured; these include variables reflective of tumor permeability such as the volume transfer constant ($K^{trans}$) from the vascular space (VS) to the extravascular-extracellular space (EES), the rate constant ($k_{ep}$) from EES to VS and the fractional volume of EES ($v_e$). A summary of a typical MR imaging protocol for the
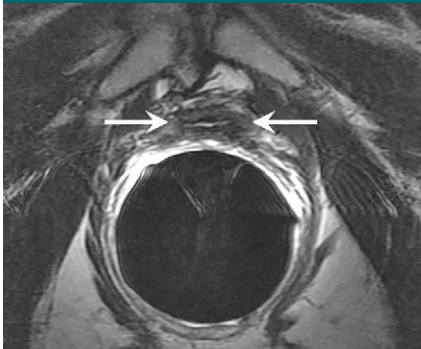
evaluation of the treated prostate is presented in the Table.
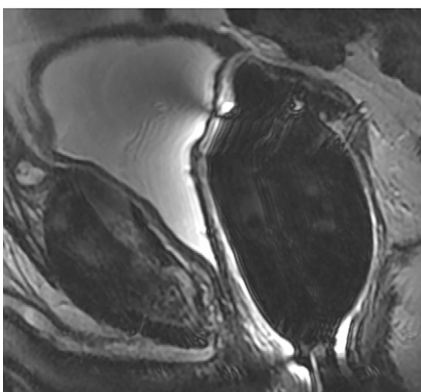
## Prostate Cancer Treatment Options

### Radical Prostatectomy

Radical prostatectomy has been performed for more than a century (14) and remains the most common treatment choice in patients with organ-confined prostate cancer (15). It involves the removal of the entire prostate, the seminal vesicles, and the ampullary portions of the vasa deferentia, with the formation of a vesicourethral anastomosis. Whenever possible, the surgical procedure is tailored to preserve the neurovascular bundles responsible for erectile function as well as the external sphincter muscle. The likelihood of simultaneous achievement of all three desired outcomes (cancer-free status, continence, and potency, sometimes called the "trifecta") after radical prostatectomy has been reported to be 60%–91% after 18–24 months (16–18). A variety of surgical techniques are used for radical prostatectomy, including perineal, retropubic, laparoscopic, and robotic approaches. Multiple reports in the literature discuss the advantages and disadvantages of each technique, but there is no definite consensus favoring one over the other in general or in any specific situations. Rather, it is widely accepted that any of these techniques is appropriate when

**Typical MR Imaging Protocol for Evaluation of the Treated Prostate**

| Sequence Parameter | T1 Weighted | T2 Weighted | DW (Echo Planar) | MR Spectroscopic Imaging | Dynamic Contrast Enhanced (Spoiled Gradient Recalled) |
|---|---|---|---|---|---|
| Echo time (msec) | 10 | 100–120 | 70–120 | 130 | 1.4 |
| Repetition time (msec) | 600–750 | 3500–6000 | 3500–6000 | 1000 | 4 |
| Field of view (cm) | 28–36 | 12–14 | 12–14 | 12 | 24 |
| Section thickness (mm) | 5 | 3 | 3 | 6.9 | 3–5 |
| Gap (mm) | 1 | 0 | 0 | 0 | 0 |
| Phase-encoding steps | 192 | 192–224 | 96–128 | 8 | 160 |
| Frequency-encoding steps | 320 | 256–416 | 96–128 | 16 | 256 |

Note.—NA = not applicable.

## Figure 1



a.



b.

**Figure 1:** T2-weighted MR images in 74-year-old man who has undergone prostatectomy. **(a)** Transverse and **(b)** sagittal images show that urinary bladder neck is pulled down and anastomosed to the membranous urethra. The normal vesicourethral anastomosis (arrows) has a uniform shape, with low signal intensity, similar to that of the urinary bladder wall, on T2-weighted images.

performed by a surgeon who is experienced in the technique (19).

*Expected MR imaging findings after radical prostatectomy.*—The bladder and levator sling descend to occupy the space created by the absent prostate (20) (Fig 1). A variable degree of low signal intensity, as compared with that of muscle, on images obtained with all sequences may be present at the site of vesicourethral anastomosis, indicating normal postoperative scarring. Increased signal intensity secondary to edema, as compared with that of muscle, may be present in the pelvic sidewall on T2-weighted images, particularly during the early stages of postoperative follow-up. Retained seminal vesicles are observed

in approximately 20% of patients after prostatectomy (21). On computed tomographic (CT) scans, retained seminal vesicles may be confused with soft-tissue recurrence; however, the vesicles are usually easily recognizable on MR images, as they tend to maintain their normal convoluted tubular appearance on T2-weighted images (Fig 2) (22). Alternatively, low signal intensity, relative to that of muscle, on both T1- and T2-weighted images, presumably as a result of fibrosis, may be seen in seminal vesicle remnants (21). Recognition of normal residual seminal vesicles is of paramount importance, because such recognition prevents biopsies for erroneous suspicion of recurrent tumor.

Some MR imaging findings may suggest the surgical technique used. A surgical incision in the lower abdominal wall and loss of the normal retropubic fat pad and dorsal venous complex are seen with the retropubic approach. Although the Denonvilliers (rectoprostatic) fascia is incised during both the retropubic and the perineal approaches, by the nature of the surgical access it is divided more posteroinferiorly with the perineal approach (23). As a result, low signal intensity (relative to that of muscle) on images obtained with all sequences in the anterior sphincter and rectal wall, indicative of normal postoperative fibrosis, is seen with both techniques but may be more prominent with the perineal approach. There are no imaging findings specific to laparoscopic or robotic techniques other than the absence of a large surgical incision or the presence of access portals in the abdominal wall.

Pelvic lymphadenectomy may be performed, but this is not mandatory, particularly in early-stage disease. Lymphoceles may occur at the site of lymphadenectomy and are found along the anatomic lymph node chains within the pelvis and paraaortic region. Lymphoceles are fluid-filled cysts without an epithelial lining and have been reported to occur in 12%–24% of patients (24). They usually become detectable 3–8 weeks after surgery but may persist for up to a year. They have low signal intensity on T1-weighted images and

## Figure 2



a.
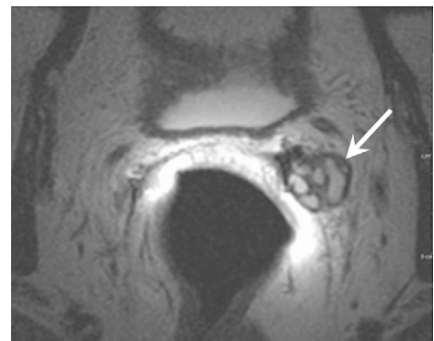


b.

**Figure 2:** Retained seminal vesicle (arrow) is seen on transverse **(a)** CT and **(b)** MR images in 64-year-old man who has undergone prostatectomy. Note that it is difficult to characterize the "lesion" (arrow) as a retained seminal vesicle on **a.** However, **b** clearly shows the typical convoluted tubular appearance of the seminal vesicle.

intermediate to high signal intensity on T2-weighted images and are typically thin-walled and unilocular and do not enhance on MR images after intravenous contrast agent administration. They should not be confused with other postoperative complications such as urinoma (direct anatomic contiguity with the urinary tract), hematoma, abscess, or necrotic lymphadenopathy (Fig 3). Metallic clips may also be visualized within the surgical field as low-signal-intensity structures on T1- and T2-weighted images. Depending on the number and distribution of the clips, the susceptibility artifact they produce may make accurate evaluation of adjacent anatomic structures extremely difficult

a.

b.

c.

d.

**Figure 3:** Transverse MR images in three patients who have undergone prostatectomy. **(a)** T2-weighted image shows bilateral pelvic sidewall lymphoceles *(L)* that compress the urinary bladder *(Bl)*. **(b)** T2-weighted image shows defect in posterior urinary bladder wall (arrow) just above the level of the vesicourethral anastomosis with an adjacent urinoma (∗). **(c)** T2-weighted and **(d)** contrast-enhanced T1-weighted images show abscess *(A)* with thick irregular walls in prostatectomy bed.
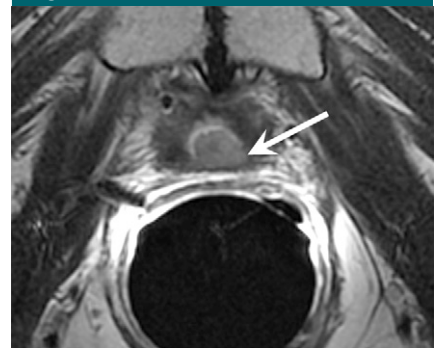


**Figure 4:** Transverse T2-weighted MR image in 59-year-old man who has undergone prostatectomy shows nodular soft-tissue mass (arrow) of intermediate to high signal intensity (compared with muscle), consistent with recurrent disease at the vesicourethral anastomosis.

and may obscure the presence of recurrence. Surgical clips are usually more conspicuous on contrast-enhanced fat-suppressed gradient-echo images than on fast spin-echo T2-weighted images.

*MR imaging features of recurrence after radical prostatectomy.*—The presence of soft tissue in the prostatectomy bed that is isointense to muscle on T1-weighted images and slightly hyperintense to muscle on T2-weighted images should be considered to be strongly suggestive of local recurrence (Fig 4). The most common site of postoperative local recurrence is the vesicourethral anastomosis around the urinary bladder and/or membranous urethra (25). Other common sites of local recurrence are retrovesical (between urinary bladder and rectum), within retained seminal vesicles, or at the anterior or lateral surgical margins of the prostatectomy bed (eg, abutting the levator ani muscles) (26). In most cases, local recurrence can be readily distinguished from normal postoperative fibrosis, which, as mentioned earlier, is of low signal intensity compared with muscle on images obtained with all sequences; however, granulation tissue may occasionally be present in the perianastomotic region, where it can mimic the appearance of tumor recurrence (26). In these circumstances, contrast-enhanced MR imaging may have a role. Recurrent tumor tends to enhance avidly in the arterial phase (Fig 5) and wash out during the venous phase, while postoperative changes tend to show either no enhancement or mild enhancement in the venous phase.

Still, we have anecdotally observed that granulation tissue and postsurgical inflammatory changes can show marked enhancement during the early postoperative period. Furthermore, recurrent tumor may show nontypical enhancement patterns, and prominent periprostatic venous plexuses may mimic the appearance of enhancing tumors.

The reported sensitivities and specificities of MR imaging for detection of local recurrence range from 48% to 100% and 52% to 100%, respectively (25–27). In one study, sensitivity and specificity, respectively, increased from 61.4% and 82.1% when using unenhanced MR imaging to 84.1% and 89.3% when using "static" MR imaging sequences acquired 20, 60, and 120 seconds after administration of intravenous contrast material (25). Casciani et al examined 46 patients after radical prostatectomy and found that sensitivity and specificity for the detection of local recurrence increased from 48% and 52% to 88% and 100%, respectively, when dynamic contrast-enhanced MR imaging was added to conventional MR imaging (27). Sciarra et al (28) reported areas under the receiver operating characteristic (ROC) curves of 0.94, 0.93, and 0.96 for MR spectroscopic imaging, dynamic contrast-enhanced MR imaging, and the combination of both, respectively, in 50 patients at high risk of local recurrence after radical prostatectomy. The analysis

of the spectroscopy data in this study was based on the choline-to-citrate ratio in regions where recurrence was suspected.

Imaging "pearls" and potential pitfalls after radical prostatectomy are summarized in Figure 6.

*Clinical management of possible recurrence after radical prostatectomy and potential impact of imaging.*—The definition of "PSA failure" after radical prostatectomy is a topic of debate. The most commonly used definition of biochemical recurrence after radical prostatectomy is a PSA level of 0.2 ng/mL or greater followed by another increased value (29,30), although some authors suggest that a PSA of 0.4 ng/mL or higher should be used to define notable biochemical failure (31). Strictly speaking, when radical prostatectomy is performed with curative intent, PSA should decrease to undetectable levels (<0.1 ng/mL) and remain low thereafter (32). PSA may fail to reach undetectable levels when, despite an organ-confined tumor, the prostatic capsule is incised or when cutting across an area of extracapsular tumor extension (33). In these cases, residual benign or malignant prostate tissue is present postoperatively and continues to produce PSA. MR imaging may be useful in this clinical scenario to help determine the amount and extent of residual prostate and to plan treatment accordingly (34). Benign residual prostate should have signal intensity similar to that of untreated prostate: that is, homogenous high signal intensity in the peripheral zone and heterogeneous signal intensity in the transition zone on T2-weighted images. When a patient's PSA level begins to increase after becoming undetectable or a nodule is palpated at digital rectal examination, cancer recurrence should be suspected.

Approximately two-thirds of men who do not receive treatment for PSA recurrence after radical prostatectomy will develop metastatic disease within 10 years (35). The greatest potential role for imaging in this context would be to identify those patients with recurrence in the prostatectomy bed who would benefit from salvage local therapy,

while sparing those with false-positive biochemical failure and those with distant metastases who would be unnecessarily exposed to the side effects and toxicities associated with local salvage treatment. The most common potentially curative form of salvage treatment after prostatectomy is RT (36). In a recent retrospective cohort study of 635 men who experienced local recurrence after radical prostatectomy (37), the investigators showed that salvage RT alone was associated with a significant three-fold increase in prostate cancer–specific survival as compared with no salvage therapy (hazard ratio, 0.32; $P < .001$). Among men who underwent salvage RT, the median radiation dose was 66.6 Gy, and the median time from recurrence to initiation of salvage RT was 1 year. The addition of hormonal therapy to salvage RT was not associated with a significant increase in prostate cancer–specific survival, and the survival benefit of salvage RT was limited to men with a PSA doubling time of less than 6 months who underwent salvage RT within 2 years of biochemical recurrence. In addition and consistent with other studies on biochemical outcome after salvage RT, the survival benefit in this study cohort was seen only among men whose PSA became undetectable after salvage RT (37).

Other less-well-studied forms of salvage treatment include cryotherapy and high-intensity focused ultrasound. In a study of 15 patients who underwent salvage cryotherapy for recurrence after radical prostatectomy, Siddiqui et al (38) reported a sustained decline in PSA in 40% of patients and disease progression in 60%. Murota-Kawano et al (39) demonstrated the feasibility of high-intensity focused ultrasound as salvage therapy in four patients. Further studies need to be performed before cryotherapy and high-intensity focused ultrasound are introduced into routine clinical practice in this context.
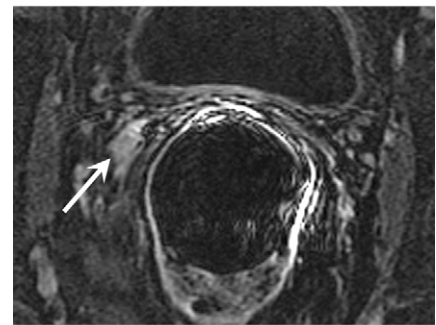
### Radiation Therapy

Other than radical prostatectomy, RT is the only form of treatment delivered with a curative intent in prostate cancer, and about 25% of patients with prostate



**Figure 5**
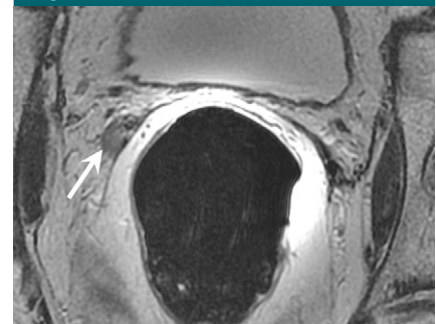
a.

b.

**Figure 5:** Transverse MR images in 76-year-old man who has undergone prostatectomy show recurrent tumor in the right seminal vesicle bed (arrow) on both **(a)** T2-weighted and **(b)** contrast-enhanced T1-weighted images. Note that recurrent tumor enhances and becomes conspicuous on **b**.

cancer undergo RT as definitive treatment (2). External-beam RT involves the use of ionizing radiation directed at the prostate and surrounding tissues through multiple portals. To minimize radiation injury to the bladder and the rectum, three-dimensional conformal RT, in which a computer alters the radiation beams to focus the radiation dose to the region of the prostate gland, has been developed (40); the most sophisticated form of three-dimensional conformal RT is called *intensity-modulated RT.* RT may also be delivered by means of brachytherapy, in which radioactive sources (seeds or needles) are implanted directly into the prostate gland and sometimes into the surrounding tissues to deliver a high dose of radiation to the tumor while sparing the bladder and the rectum as much as possible (Fig 7). The most commonly used permanent implants are iodine 125 or palladium 103 seeds.

## Figure 6

### After Radical Prostatectomy

| **Imaging Pearls** | **Potential Pitfalls** |
|---|---|
| The typical appearance of recurrence is a soft-tissue nodule in the prostatectomy bed that is isointense to muscle on T1-weighted and slightly hyperintense to muscle on T2-weighted images | Retained seminal vesicles may mimic soft tissue recurrence |
| | Metallic clips (low signal intensity on T1- and T2-weighted images) may interfere with evaluation |
| Differential diagnosis: postoperative fibrosis (low signal intensity on images from all sequences) and granulation tissue (may mimic signal intensity of tumor recurrence) | "Residual prostate" after prostatectomy: PSA does not reach undetectable levels. Residual prostate should not be confused with recurrence (although malignant cells may be present in residual tissue) |
| | Prominent periprostatic venous plexus should not be confused with "enhancing" recurrent tumor |
| Intravenous contrast material is helpful because tumor tends to enhance earlier and more avidly than do postoperative changes | Differential diagnosis of postoperative collections:<br>• Lymphocele: well-defined, thin walls, homogeneous contents, mild or no wall enhancement, no surrounding inflammatory changes<br>• Abscess: thick walls, internal septations, heterogeneous contents, marked wall enhancement, surrounding inflammatory changes<br>• Hematoma: contains blood-degradation products<br>• Urinoma: direct contiguity with the urinary tract |

**Figure 6:**   Pearls and pitfalls of imaging after radical prostatectomy.

## Figure 7



**Figure 7:**   Transverse T2-weighted MR image in 62-year-old man shows multiple radioactive seeds (arrow) implanted in the prostate. There is also decreased signal intensity throughout the prostate with loss of zonal differentiation.
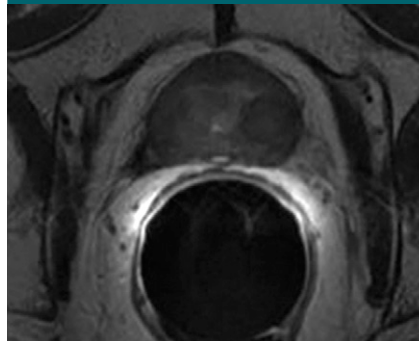
## Figure 8



**Figure 8:**   Transverse T2-weighted MR image in 78-year-old man who has undergone external-beam RT shows decreased signal intensity throughout prostate, with loss of zonal differentiation.

*Expected MR imaging findings after RT.*—After radiation therapy, the entire prostate and the seminal vesicles show decreased size and diffusely decreased signal intensity on T2-weighted images, and the peripheral, central, central, and transition zones appear less distinct from each other (Fig 8) (41,42). Prostate tumors also show changes, which may include decreased size, reduced capsular bulging, capsular irregularity, or decreased extracapsular extension. These changes are caused by RT-induced glandular atrophy and fibrosis. Despite higher radiation dosages used in modern techniques, dose modulation limits the toxicity to the bladder, urethra, and rectum. The effects of RT on the T2-weighted imaging appearance of adjacent anatomic structures include increased wall thickness, increased signal intensity in the bladder and/or rectal wall, thickening of the perirectal fascia, and increased signal intensity of

the pelvic sidewall musculature (41). In addition, there may be increased signal intensity in the bone marrow on T1-weighted images due to post-RT fatty replacement (41). MR imaging can also be used for evaluating seed distribution and demonstrating treatment-related changes after brachytherapy (42).

*Recurrence after RT.*—The first important aspect to consider when evaluating possible recurrence after RT is that recurrence tends to occur at the site of the primary (pre-RT) tumor (43,44). Despite the frequent overall decrease in glandular signal intensity after RT, malignant tumors are still most often recognized as lesions of confluent signal intensity that is relatively lower than that of surrounding noncancerous prostate (Fig 9), much as they are in the untreated prostate (45). The relative signal intensity difference between treated gland and cancerous lesion is typically less than that in the untreated gland, however, often making the lesions less conspicuous. In addition, a focal hypointense region on T2-weighted images may represent treated tumor and not necessarily cancer recurrence, and recurrent tumors may not be apparent on T2WI. In these situations, there may be a role for multiparametric assessment with MRSI,

DW-MR imaging and DCE-MR imaging (Figs 10–12). In a study to evaluate prostate cancer recurrence after radiation therapy, spectroscopy was more sensitive than conventional MR imaging and digital rectal examination (77% versus 68% and 16%, respectively), though it was also much less specific (78% versus >90% for both MR imaging and digital rectal examination) (46), probably as a result of metabolic alterations in benign tissue after RT. In a study of 64 men suspected of having recurrence after definitive external-beam RT, Westphalen et al (47) showed that use of combined T2-weighted and MR spectroscopic imaging (area under the receiver operating characteristic curve = 0.79), as compared with use of T2-weighted imaging alone (area under the curve = 0.67), significantly improved the detection of local recurrence ($P$ = .001). Dynamic contrast-enhanced MR imaging has also been reported to improve the detection of recurrence after RT by showing early arterial enhancement of tumor nodules and early washout (48,49). In addition, Kim et al (50) reported that the area under the curve for predicting recurrence after RT improved from 0.61 with T2-weighted imaging to 0.88 when DW MR imaging was added to T2-weighted imaging ($P$ < .01). In a preliminary report on the use of multiparametric MR imaging in patients suspected of having recurrence after RT, Akin et al (51) recently reported that the area under the curve for two readers increased from 0.64 and 0.53 when using T2-weighted imaging in isolation to 0.95 and 0.86 when using the combination of T2-weighted, DW, and dynamic contrast-enhanced MR imaging.

Imaging pearls and potential pitfalls after RT are summarized in Figure 13.

*Clinical management of suspected recurrence after RT and the potential impact of imaging.*—The clinical assessment of recurrence after RT is challenging. First of all, PSA levels decrease slowly after radiation (52) and may never reach undetectable levels. The time to reach nadir (lowest PSA value) after RT is variable (up to years) and depends on factors such as radiation
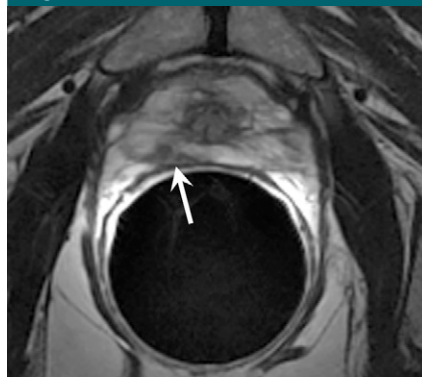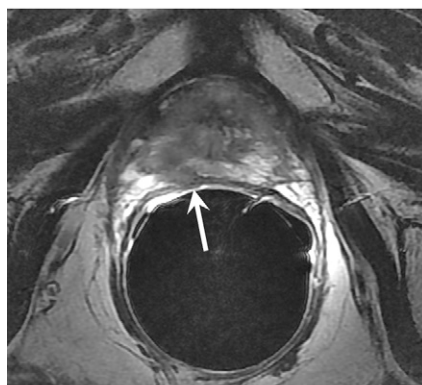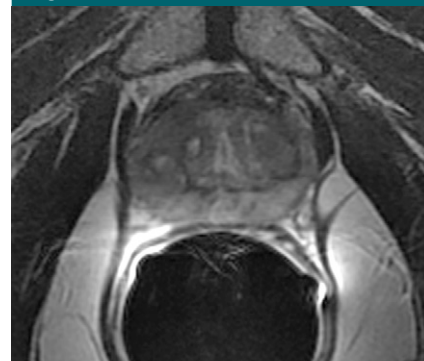
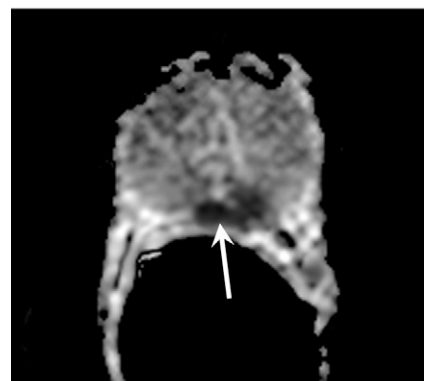**Figure 9:** Transverse T2-weighted MR images obtained **(a)** before and **(b)** 2 years after external-beam RT. **(a)** Focal tumor (arrow) is shown in right peripheral zone at apex of the prostate. **(b)** Recurrent mass with extracapsular extension (arrow) can be seen at site of original tumor, which was biopsy-proved prostate cancer recurrence.

dose, prostate size, and pretreatment PSA level. Furthermore, approximately one-third of patients experience a PSA "bounce" (defined as a PSA increase of at least 0.4 ng/mL, followed by a PSA decrease) after RT (53), which further confounds the ongoing debate about the most accurate interpretation of serial PSA monitoring. Preliminary data suggest that MR imaging or MR spectroscopic imaging may be helpful in this situation. A recent study with 24 patients who fulfilled the criteria for a PSA bounce (54) showed that the choline-plus-creatine signal, although markedly reduced, was observable after brachytherapy. The authors concluded that these findings support the benign

**Figure 10:** MR imaging in 70-year-old patient with increasing PSA level following RT. **(a)** Transverse T2-weighted MR image shows no suspicious areas. **(b)** ADC map in same patient shows area of restricted diffusion consistent with tumor (arrow). Recurrent tumor at this location was confirmed at biopsy.

nature of the PSA bounce and could potentially be used in the assessment of recurrence after brachytherapy. Still, defining biochemical recurrence after RT remains a complex issue. Currently, the Phoenix definition is the most widely used. It was introduced in 2006 by the Radiation Therapy Oncology Group–American Society for Therapeutic Radiology and Oncology and defines biochemical recurrence as an absolute increase in PSA level of 2 ng/mL or greater above the nadir (55). Once biochemical failure is established, the next step is differentiation of local from distant metastatic recurrence. The interpretation of prostate biopsies after RT, commonly proposed as the reference standard for detection of local recurrence, is also complicated and thus not
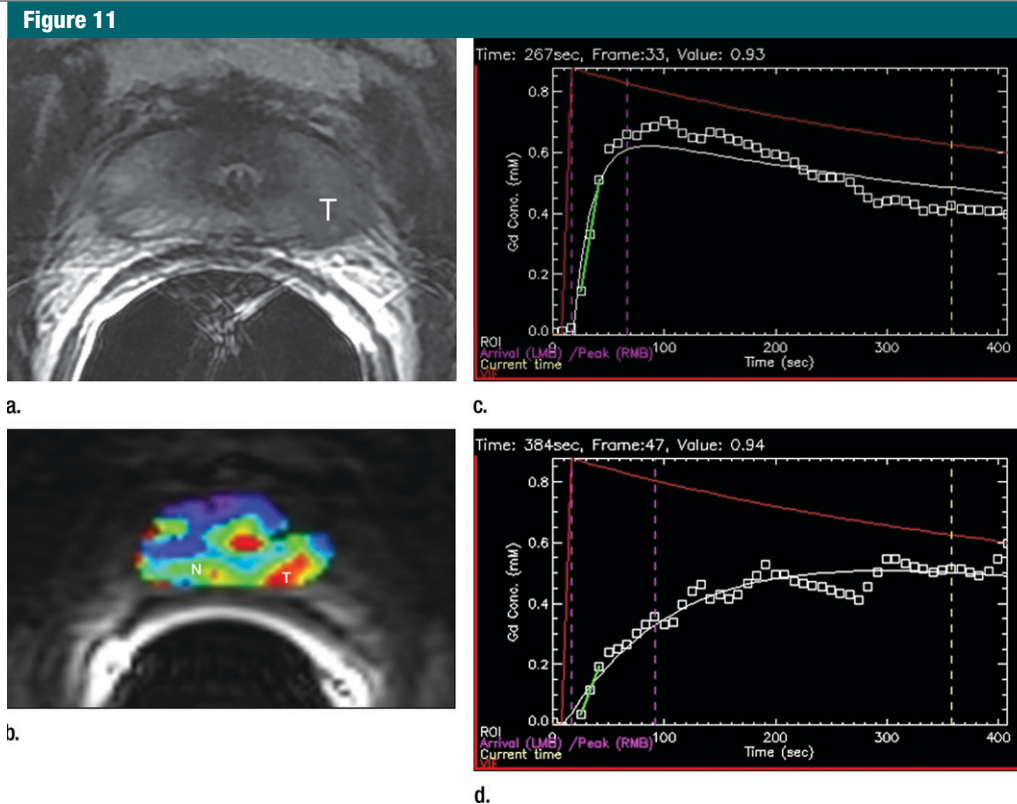
**Figure 11:** Biopsy-confirmed prostate cancer recurrence in left peripheral zone in 72-year-old patient after external-beam RT. **(a)** Transverse T2-weighted MR image shows area suspicious for tumor recurrence *(T)*, but the possibility of normal post-treatment change cannot be excluded. **(b)** $K^{trans}$ map from axial dynamic contrast-enhanced MR imaging shows increased enhancement in area suspicious for tumor recurrence *(T)*, compared with area of normal prostate tissue *(N)*. **(c, d)** Contrast enhancement–time curves generated from dynamic contrast-enhanced MR imaging data show rapid avid enhancement in **(c)** region suspicious for tumor, as compared with **(d)** normal prostate tissue.

routinely recommended in all patients with increasing PSA level after RT. In addition to false-negative results due to sampling error, false-positive results may also occur, because the presence of malignant cells in biopsy specimens may not represent biologically active tumors, especially in the first 1–2 years after RT (52,56). Authors of some studies suggest that the rate of PSA increase (including the PSA doubling time and time to PSA failure) may be the most important predictor of the presence of distant metastases (57,58). The goal of MR imaging in this setting is confident identification of recurrence for targeted or whole-gland salvage therapies, as well as staging to determine suitability of one salvage therapy versus another.

The most studied local salvage treatment option is radical prostatectomy, with 5-year disease-free survival reported at 47%–67% (59–63). The benefit of salvage prostatectomy must be balanced against the risks of subsequent toxicity effects such as bladder contracture, urinary incontinence, and rectal injuries. These risks are greater in the setting of salvage prostatectomy than in the de novo setting because of radiation-induced changes in the surgical field. RT may induce fibrosis, merging of tissue planes used for dissection, and poorer wound healing.

Salvage cryotherapy also has a role in the management of localized recurrence after RT, especially in older patients and those with some comorbidities (64). The reported 5-year biochemical disease-free survival after salvage cryotherapy ranges from 23% to 58% (65–68). Side effects of salvage

cryoablation are more prevalent and serious compared with those noticed in cases of primary intent (64). Although earlier studies reported a urinary incontinence rate as high as 72% (66), the urinary incontinence rate in recent series ranges from 4.3% to 6.7% (65,69). The risk of complications seems to be higher after transurethral surgery or in the presence of bulky disease (65). To decrease the rates of morbidity, Eisenberg and Shinohara (70) proposed to reduce the treated volume of the prostate by applying a partial salvage procedure.

Salvage brachytherapy is also a feasible option, with 5-year disease-free survival reported at 20%–67% (71–73). One important difficulty regarding salvage brachytherapy remains dose determination, since repeat irradiation

increases the risk of radiation-induced toxicity. The choice of radiation dose that offers the best balance between efficacy and toxicity remains complex (64).

The use of high-intensity focused ultrasound has also been studied in the context of post-RT recurrence. The largest published series of salvage high-intensity focused ultrasound to date from Murat et al (74) included 167 patients treated between 1995 and 2006. The authors reported 3-year progression-free survival rates of 53%, 42%, and 25% for low-, intermediate-, and high-risk patients, respectively. No rectal complications were observed, but 11% of patients required a urinary sphincter implantation. Complications reported in the recent literature include rectal fistulas, urethral strictures, and bladder neck contracture (75,76).

### Androgen-Deprivation Therapy

Androgen-deprivation therapy has long been used to treat advanced prostate cancer. In 1941, Huggins and Hodges (77) first noted the beneficial effects of castration and injection of estrogens in patients with metastatic prostate cancer. More recently, androgen-deprivation therapy has been used in additional clinical settings, such as in patients with increasing PSA levels after local treatment or as adjunct therapy for men undergoing RT for locally advanced disease (78). Androgen deprivation may be performed surgically (bilateral orchiectomy) or pharmacologically using gonadotropin-releasing hormone agonists (leuprolide, goserelin), gonadotropin-releasing hormone antagonists, antiandrogen drugs (ketoconazole), androgen receptor antagonists (flutamide, bicalutamide, and nilutamide) or 5α-reductase inhibitors (finasteride) (79).

*Expected MR imaging findings after androgen-deprivation therapy.*—At MR imaging and MR spectroscopic imaging, patients demonstrate diverse morphologic and metabolic responses to androgen-deprivation therapy, with the magnitude of responses depending on the type (single therapy or combined agents) and duration of therapy. The
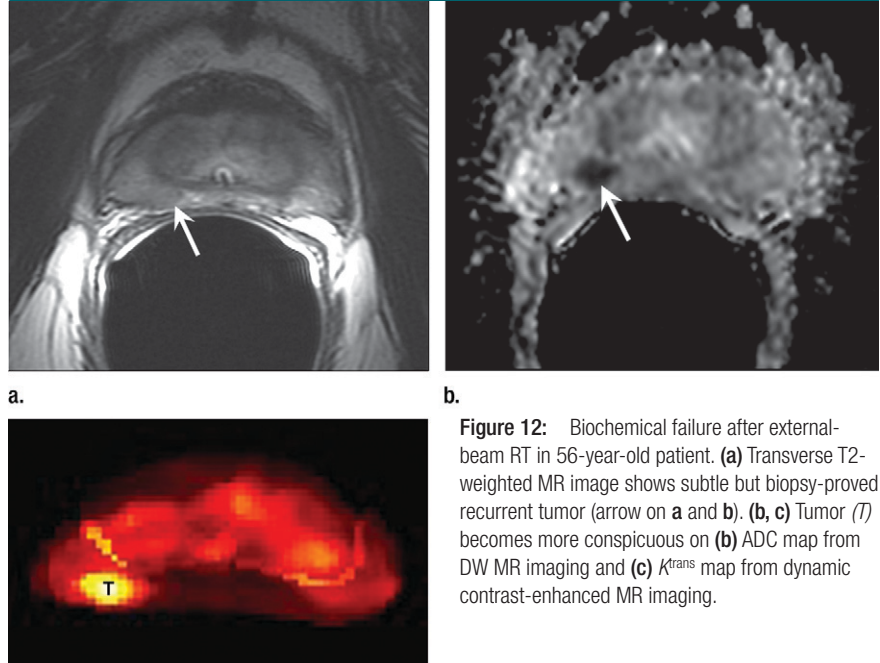
**Figure 12**



a.



b.



c.

**Figure 12:** Biochemical failure after external-beam RT in 56-year-old patient. **(a)** Transverse T2-weighted MR image shows subtle but biopsy-proved recurrent tumor (arrow on **a** and **b**). **(b, c)** Tumor *(T)* becomes more conspicuous on **(b)** ADC map from DW MR imaging and **(c)** $K^{trans}$ map from dynamic contrast-enhanced MR imaging.

findings range from no morphologic or metabolic changes with short duration monotherapy (80) to homogeneously reduced signal intensity on T2-weighted images and substantial loss of the prostatic metabolites choline, creatine, and citrate at MR spectroscopic imaging, resulting in complete loss of all observable metabolites (total metabolic atrophy) in about a quarter of patients who undergo androgen-deprivation therapy for more than 16 weeks (Fig 14) (81). A decrease in prostate volume is observed, which occurs to a greater extent in the peripheral zone than in the transition zone (82). The seminal vesicles also decrease in size and demonstrate low signal intensity (lower than that of fat but higher than that of adjacent muscle) on T2-weighted images (83).

*Recurrence after androgen-deprivation therapy.*—Androgen-deprivation therapy may reduce the volume of tumors but not necessarily result in downstaging of prostate cancer. A recent study by D'Amico et al (84) showed that prostate tumor volume changes on 1.5-T endorectal MR images during neoadjuvant androgen-

suppression therapy may be predictive of prostate cancer recurrence in men treated with RT. Because of the varying degrees of decreased signal intensity in the peripheral zone, differentiation between tumor and posttreatment change is difficult, and the presence of tumor may be overestimated (82). Despite this, in our experience the tumor can be readily identified on T2-weighted images in most cases (Fig 15). At MR spectroscopic imaging, citrate levels decrease faster than choline and creatine levels during androgen-deprivation therapy. As a result, the mean choline-plus-creatine–to-citrate ratio increases in both normal and malignant tissue with increasing therapy duration (80). The total metabolic atrophy mentioned earlier occurs more frequently in normal peripheral zone tissue than in cancerous tissue. For a short time after therapy, therefore, metabolic atrophy may be useful as a substitute marker for normal tissue when the choline-plus-creatine–to-citrate ratio cannot be determined owing to low metabolite levels (80). However, with increasing therapy duration,

Radiology

### Figure 13

**After RT**

**Imaging Pearls**

Hallmarks of prior pelvic irradiation include high signal intensity on T2-weighted images and/or thickening of the bladder, rectal wall, perirectal fascia, and pelvic sidewall muscles, as well as hyperintense bone marrow on T1-weighted images owing to fatty replacement

The main effects of RT on the MR imaging appearance of the prostate are a decrease in size and diffusely decreased signal intensity on T2-weighted images

Recurrent tumor typically appears on T2-weighted images as a nodular lesion of lower signal intensity than the adjacent normal prostate, in the same location as the pre-RT tumor; other identifying features include growth of the lesion and progressive bulging of the prostatic capsule over time

Restricted diffusion on DW MR images and rapid contrast agent uptake and washout on dynamic contrast-enhanced MR images favor the presence of recurrence

**Potential Pitfalls**

Focal regions of hypointensity in the prostate on T2-weighted images may represent treated tumor and not necessarily cancer recurrence

Recurrent tumors may not be apparent on T2-weighted images

RT-induced capsular irregularity may hinder evaluation of extracapsular extension

**Figure 13:** Pearls and pitfalls of imaging after RT.

metabolic atrophy is also observed prominently in malignant tissue (80). Overall, the inherent variability of changes induced in both benign and malignant prostate tissue depending on the type, duration, and dose of androgen-deprivation therapy limit the clinical usefulness of MR imaging and MR spectroscopic imaging in these patients.

Imaging pearls and potential pitfalls after androgen deprivation therapy are summarized in Figure 16.

*Clinical management of suspected recurrence after androgen-deprivation therapy and the potential impact of imaging.*—Although androgen-deprivation therapy may slow disease progression, it is not considered a curative treatment. In a study with 626 patients who had advanced local or metastatic prostate cancer treated with androgen-deprivation therapy, 231 had evidence of disease progression after a median follow-up of 51 months (85). Nakata et al (86) analyzed the prognostic factors of prostate cancer that responds well initially to maximal androgen blockade but later shows PSA relapse and is treated with estrogen; they found that the factor that most notably affected prognosis after estrogen therapy was PSA response 3 months after initiation of estrogen therapy (hazard ratio, 12.61) followed by PSA doubling time at estrogen therapy (hazard ratio, 2.59).
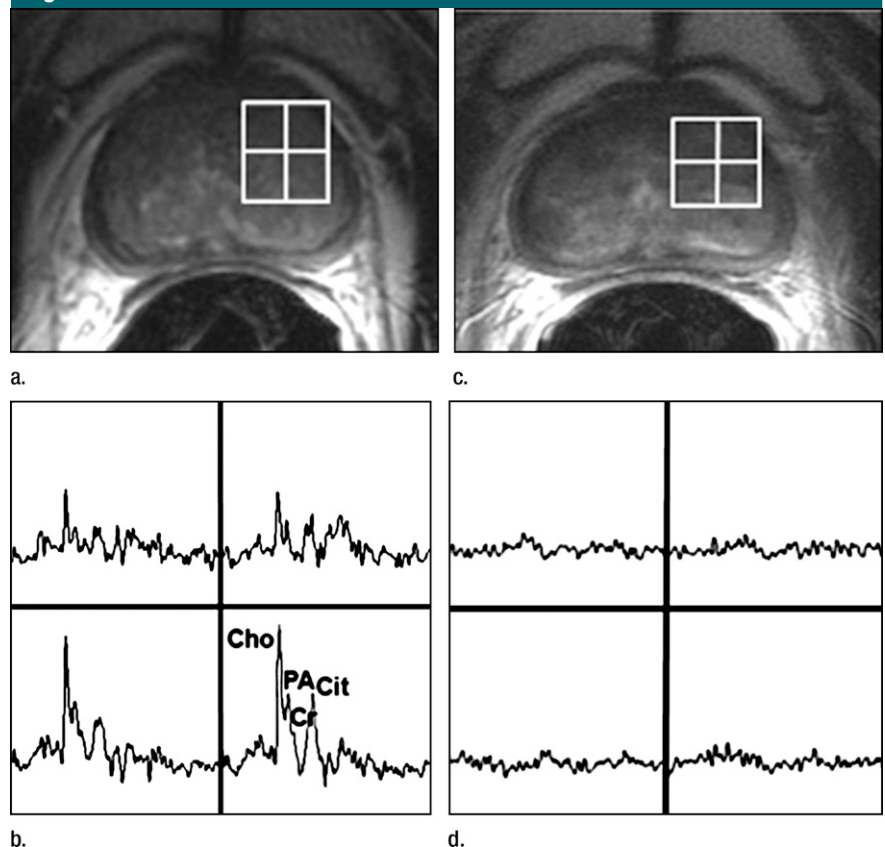
### Figure 14



**Figure 14:** Prostate cancer in 77-year-old patient. **(a)** Pretreatment MR spectroscopic imaging spectral grid overlaid on T2-weighted MR image. **(b)** MR spectroscopic imaging spectra show choline *(Cho),* polyamine *(PA),* citrate *(Cit),* and creatine *(Cr)* peaks. Voxels in spectral grid with elevated choline and reduced citrate are suspicious for cancer. **(c)** At 18 months after hormone therapy and RT, spectral grid overlaid on T2-weighted image at a similar level is shown. **(d)** MR spectroscopic imaging peaks show no metabolites (metabolic atrophy).

## Figure 15
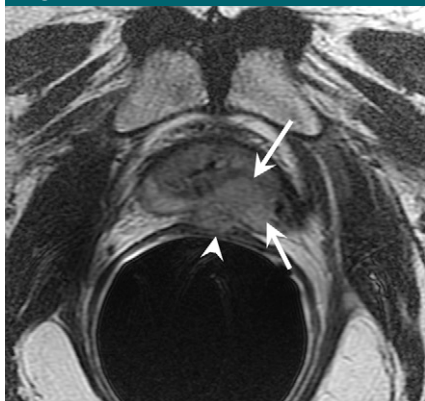


a.
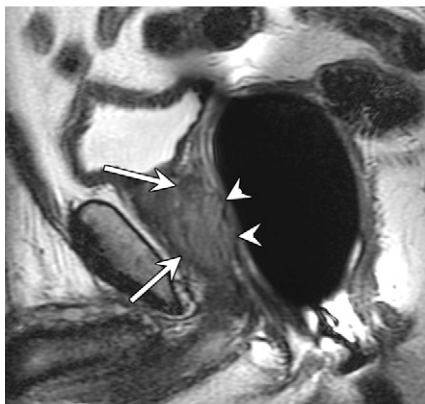


b.

**Figure 15:** Increasing PSA level after androgen-deprivation therapy in 81-year-old patient. **(a)** Transverse and **(b)** sagittal T2-weighted MR images show recurrent tumor (arrows) extending from left base to apex, with extracapsular extension and involvement of the rectal wall (arrowheads).

Some authors suggest that given the potential toxicities (increased risk of skeletal fracture, incident diabetes, cognitive impairment, and cardiovascular-related morbidity) and costs, particularly in older men with recurrence after primary treatment of prostate cancer, observation may represent a better alternative, although patient anxiety often leads to an earlier initiation of androgen-deprivation therapy (87). In this context, MR imaging may be useful to assess the changes in volume and extent of prostate cancer recurrence and hence be of value when deciding between further androgen-deprivation therapy or observation only.

## Figure 16



| After Androgen-Deprivation Therapy | |
| --- | --- |
| **Imaging Pearls** | **Potential Pitfalls** |
| The imaging features of the prostate after androgen-deprivation therapy may be similar to those after radiation therapy (decreased volume, decreased signal intensity on T2-weighted images, loss of zonal differentiation); however, radiation therapy–induced changes in adjacent structures are absent | Findings vary, depending of the type and duration of androgen-deprivation therapy

Differentiation between treated and recurrent tumor may be difficult after androgen-deprivation therapy in the same way that it is difficult after radiation therapy |

**Figure 16:** Pearls and pitfalls of imaging after androgen-deprivation therapy.

### Focal Therapies

1. Cryotherapy consists of the ablation of tissue by extremely cold temperatures. It has been used to treat prostate cancer since the 1960s, and the initial reported survival rates were similar to those for conventional therapies (88). However, serious complications, including fistula formation and urethral sloughing, occurred relatively commonly, and the procedure was largely abandoned (89). Later modifications in cryosurgical equipment and technique, such as urethral warming, percutaneous cryoprobe placement, and transrectal ultrasonographic (US) monitoring, have decreased the associated morbidity rate, and there has recently been a resurgence of interest in this procedure. Currently, cryotherapy is a recognized form of treatment for localized prostate cancer, although further clinical trials are necessary to demonstrate its effectiveness (90).

2. High-intensity focused ultrasound causes coagulation necrosis in the targeted tissue by converting mechanical energy into heat and generating a cavitation effect. This procedure is a valuable alternative in the management of low- and intermediate-risk localized prostate cancer and of local recurrence after external-beam RT (91,92). Its major imitations are the difficulty in ablating the entire prostate, especially in a large (>40-g) gland and difficulty in treating anterior tumors (90).

3. Photodynamic therapy enables destruction of targeted tissues by using a light-sensitive agent (photosensitizer)

and laser light of a specific wavelength in the presence of oxygen. The photosensitizer absorbs the light and transfers the energy to adjacent oxygen molecules, creating reactive oxygen species that trigger cell destruction (93,94). Photodynamic therapy for prostate cancer is performed with US-guided transperineal placement of illuminating laser fibers by using an approach similar to that of brachytherapy (90).

*Expected MR imaging findings after focal treatments.*—Focal treatments may be used to treat the entire prostate or to target specific prostate regions and can be delivered by using a transrectal or transperineal approach and with US or MR guidance (95,96). Depending on the extent of the treatment, loss of zonal differentiation, thickening of the prostatic capsule, and periprostatic fibrosis and scarring may be present (Fig 17). When delivered via a transrectal approach, the anterior regions of the base of the prostate may be more difficult to target, depending on the size of the prostate and the degree of tissue penetration of each technique. After cryotherapy, heterogeneous enhancement intermixed with areas of necrosis and thickening of the prostatic capsule, urethra, and rectal wall are seen on T1-weighted images (97).

After high-intensity focused ultrasound, ablation-induced changes in the region of the lesions appear on contrast-enhanced T1-weighted images as unenhanced hypointense regions with 3–8-mm-thick peripheral rims of enhancement that resolve within 3–5 months (98). Kirkham et al (99) showed that
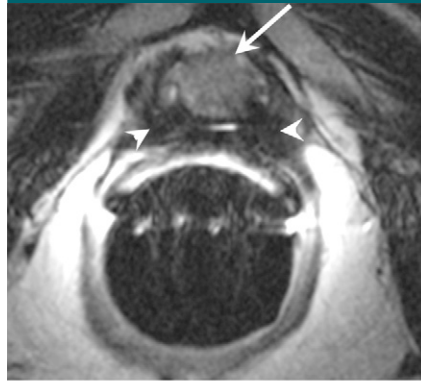
**Figure 17**

a.
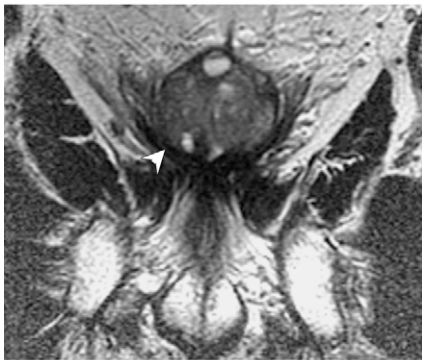
b.

**Figure 17:** **(a)** Transverse and **(b)** coronal T2-weighted MR images in 59-year-old patient treated with high-intensity focused ultrasound shows thickened prostatic capsule (arrow) and extensive tissue fibrosis around the prostate (arrowhead). There is diffusely decreased volume in the peripheral zone with benign prostatic hyperplasia in the transition zone.

**Figure 18**

a.

b.

**Figure 18:** Transverse **(a)** T2-weighted and **(b)** contrast-enhanced T1-weighted MR images in 56-year-old patient with increasing PSA level after cryotherapy show recurrent tumor (arrow) Note that tumor has intermediate signal intensity on **a** and is markedly enhanced on **b**. Postcryotherapy fibrosis (arrowheads) demonstrates low-signal-intensity on **a** and does not enhance on **b**.

**Figure 19**

a.

b.

**Figure 19:** Transverse **(a)** T2-weighted and **(b)** contrast-enhanced T1-weighted MR images in 60-year-old patient with increasing PSA level after high-intensity focused ultrasound show recurrent tumor (arrow) with intermediate signal intensity relative to that of muscle on **a** and enhancement on **b**. After treatment, defect (arrowhead) and surrounding fibrosis are also seen.
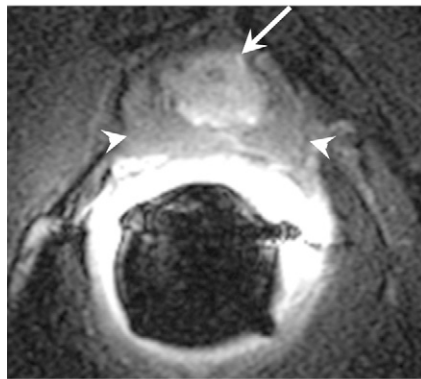
at 6 months, the prostate is of predominantly low signal intensity on T2-weighted images and that there is a median volume reduction of 61%. Kirkham et al also concluded that the volume of prostate tissue enhancing on the initial posttreatment image correlated well with serum PSA level nadir (Spearman $r = 0.90$, $P < .001$) and with volume at 6 months (Pearson $r = 0.80$, $P = .001$) (99).

After photodynamic therapy, MR imaging may be used to assess the extent and distribution of the expected necrosis in the target region. In one study (100), most patients showed marked irregularity at the treatment boundary that was best appreciated on T1-weighted images after intravenous
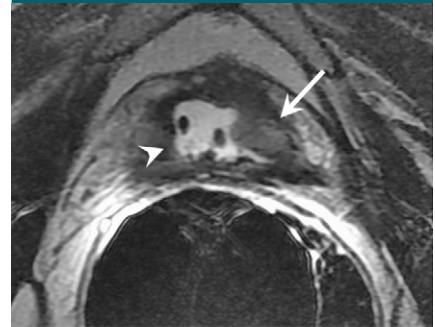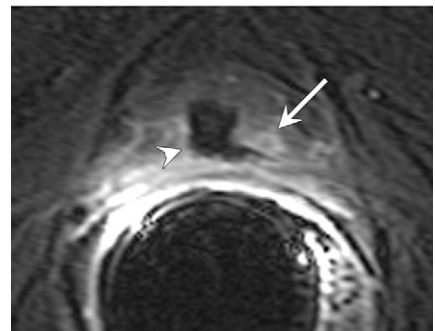
administration of contrast material, with areas of enhancement (viable tissue) interposed between nonenhancing low-signal-intensity regions (necrosis).

*Recurrence after focal treatments.—* In general, enhancing soft-tissue lesions after focal treatments should be considered suggestive of recurrence, just as they are after other forms of treatment. It is important to be aware that recurrent lesions may present in conjunction with normal posttreatment appearances (Figs 18, 19). Furthermore, the characteristics typically associated with recurrence on T2-weighted images may not represent recurrence in some cases, and in some cases of recurrence,

these features simply fail to appear (97). Some authors suggest that MR spectroscopic imaging is superior to MR imaging with regard to differentiation cancer voxels from necrosis voxels (101), but at present MR spectroscopic imaging is not widely used to aid clinical decision making. In one study, postoperative contrast-enhanced MR imaging up to 3 weeks after surgery was used in an attempt to predict the success of cryoablation, as determined with tissue sample results at 6 months after treatment and follow-up PSA levels; however, no significant correlations were found between MR imaging findings, biopsy results and PSA levels (102).

After high-intensity focused ultrasound, the detection of recurrent or residual disease may be hindered by diffuse or multifocal areas of low signal

Radiology

## Figure 20



### After Focal Therapies

**Imaging Pearls**

The site of treatment-related changes should correlate to the region of the prostate targeted by the focal therapy

Intravenous contrast material is recommended for differentiating treatment-induced focal necrosis from viable tissue

**Potential Pitfalls**

It may be difficult to differentiate viable tumor from reactive enhancing prostate tissue, particularly at the margins of the treated area.

**Figure 20:** Pearls and pitfalls of imaging after focal therapies.

intensity on T2-weighted MR images (98). A short time to peak enhancement, early washout, and other pharmacokinetic parameters observed on dynamic contrast-enhanced MR images in patients with untreated prostate cancer can also be present in cases of recurrence after high-intensity focused ultrasound (101). A recent study showed that for prediction of local tumor progression of prostate cancer after high-intensity focused ultrasound, dynamic contrast-enhanced MR imaging was more sensitive but less specific than the combination of T2-weighted and DW MR imaging (103). In a study by Rouvière et al (104) on the use of T2-weighted and dynamic contrast-enhanced MR imaging in 59 patients suspected of having recurrence after high-intensity focused ultrasound, the odds ratio of the probability of finding viable cancer and viable prostate tissue (benign or malignant) during routine biopsy was 1.38; this odds ratio increased to 3.35 when biopsies were targeted at lesions identified on T2-weighted and dynamic contrast-enhanced MR images.

Imaging pearls and potential pitfalls after focal treatments are summarized in Figure 20.

*Clinical management of possible recurrence after focal treatments and the potential impact of imaging.*—There is no definite consensus about how to define failure after focal treatment. After whole-gland cryotherapy, serum PSA levels initially increase sharply due to the release of intracellular PSA associated with cellular necrosis (105). The PSA nadir is generally reached in 3 months (106). However, serum PSA levels after cryotherapy may not decrease to

an undetectable level because of the necessary preservation of a thin rim of periurethral tissue for whole-gland ablation or from a more substantial spared portion of the gland with subtotal treatment. Although data have shown that a lower PSA nadir is associated with an increased chance of a stable PSA level and negative biopsy results (eg, residual cancer is rarely found among patients with a PSA nadir of less than 0.5 ng/mL) (107), the actual PSA nadir level that should be achieved after cryotherapy is unknown (108,109). After whole-gland high-intensity focused ultrasound the PSA nadir is observed at around 6 months (110).

When attempting to establish biochemical failure after focal therapies, some investigators use static PSA cutoff values such as 0.3, 0.4, 0.5, and 1.0 ng/mL, while others choose to follow the Phoenix (PSA nadir + 2) definition (55). Given the lack of evidence for standardized definitions of biochemical recurrence, many centers routinely perform prostate biopsy at different time points after focal therapies. The results of conventional and advanced MR imaging techniques in detecting recurrence after local therapies, discussed earlier in this article, are encouraging, and it is hoped that these techniques may one day prevent unnecessary biopsies after focal therapies; however, further studies are required before these techniques can be widely adopted for evaluating recurrence after focal therapy. Once recurrence is confirmed, focal therapies may be repeated (111,112). Bahn et al (111) performed a second round of therapy in 32 patients with positive biopsy results after primary cryotherapy. Reported PSA-recurrence-free survival

rates at 63 months were 68%, 72%, and 91% using variable definitions of failure of 0.5 ng/mL, 1.0 ng/mL, and the American Society for Therapeutic Radiology and Oncology criteria (PSA nadir + 2), respectively. Salvage external-beam RT is also a possible management option for recurrent prostate cancer following initial focal therapy.

## Conclusion

Many treatment options are available to patients with newly diagnosed prostate cancer. MR imaging plays an important role not only in initial staging of prostate cancer, but also when there is clinical or biochemical suspicion of residual or recurrent disease after treatment. All forms of treatment alter the MR imaging features of the prostatic region to a greater or lesser extent; by recognizing typical posttreatment appearances and distinguishing them from the features of recurrent or residual cancer, the radiologist can aid subsequent clinical management.

### References

1. Jemal A, Siegel R, Xu J, Ward E. Cancer statistics, 2010. CA Cancer J Clin 2010;60(5):277–300. [Published correction appears in CA Cancer J Clin 2011;61(2):133–134.]

2. Cooperberg MR, Broering JM, Carroll PR. Time trends and local variation in primary treatment of localized prostate cancer. J Clin Oncol 2010;28(7):1117–1123.

3. Akin O, Hricak H. Imaging of prostate cancer. Radiol Clin North Am 2007;45(1):207–222.

4. Costello LC, Franklin RB. The intermediary metabolism of the prostate: a key to understanding the pathogenesis and progression of prostate malignancy. Oncology 2000;59(4):269–282.

5. Costello LC, Franklin RB. Novel role of zinc in the regulation of prostate citrate

metabolism and its implications in prostate cancer. Prostate 1998;35(4):285–296.

6. Kaji Y, Kurhanewicz J, Hricak H, et al. Localizing prostate cancer in the presence of postbiopsy changes on MR images: role of proton MR spectroscopic imaging. Radiology 1998;206(3):785–790.

7. Podo F, de Certaines JD. Magnetic resonance spectroscopy in cancer: phospholipid, neutral lipid and lipoprotein metabolism and function. Anticancer Res 1996;16(3B):1305–1315.

8. Ackerstaff E, Pflug BR, Nelson JB, Bhujwalla ZM. Detection of increased choline compounds with proton nuclear magnetic resonance spectroscopy subsequent to malignant transformation of human prostatic epithelial cells. Cancer Res 2001;61(9):3599–3603.

9. Shukla-Dave A, Hricak H, Moskowitz C, et al. Detection of prostate cancer with MR spectroscopic imaging: an expanded paradigm incorporating polyamines. Radiology 2007;245(2):499–506.

10. Jung JA, Coakley FV, Vigneron DB, et al. Prostate depiction at endorectal MR spectroscopic imaging: investigation of a standardized evaluation system. Radiology 2004;233(3):701–708.

11. Westphalen AC, Coakley FV, Qayyum A, et al. Peripheral zone prostate cancer: accuracy of different interpretative approaches with MR and MR spectroscopic imaging. Radiology 2008;246(1):177–184.

12. Charles-Edwards EM, deSouza NM. Diffusion-weighted magnetic resonance imaging and its application to cancer. Cancer Imaging 2006;6:135–143.

13. Tofts PS, Brix G, Buckley DL, et al. Estimating kinetic parameters from dynamic contrast-enhanced T(1)-weighted MRI of a diffusable tracer: standardized quantities and symbols. J Magn Reson Imaging 1999;10(3):223–232.

14. Young HH. VIII. Conservative perineal prostatectomy: the results of two years' experience and report of seventy-five cases. Ann Surg 1905;41(4):549–557.

15. Cooperberg MR, Lubeck DP, Meng MV, Mehta SS, Carroll PR. The changing face of low-risk prostate cancer: trends in clinical presentation and primary management. J Clin Oncol 2004;22(11):2141–2149.

16. Bianco FJ Jr, Scardino PT, Eastham JA. Radical prostatectomy: long-term cancer control and recovery of sexual and urinary function ("trifecta"). Urology 2005;66(5 Suppl):83–94.

17. Eastham JA, Scardino PT, Kattan MW. Predicting an optimal outcome after radical prostatectomy: the trifecta nomogram.

J Urol 2008;179(6):2207–2210; discussion 2210–2211.

18. Patel VR, Coelho RF, Chauhan S, et al. Continence, potency and oncological outcomes after robotic-assisted radical prostatectomy: early trifecta results of a high-volume surgeon. BJU Int 2010;106(5):696–702.

19. Scolieri MJ, Resnick MI. The technique of radical perineal prostatectomy. Urol Clin North Am 2001;28(3):521–533.

20. Allen SD, Thompson A, Sohaib SA. The normal post-surgical anatomy of the male pelvis following radical prostatectomy as assessed by magnetic resonance imaging. Eur Radiol 2008;18(6):1281–1291.

21. Sella T, Schwartz LH, Hricak H. Retained seminal vesicles after radical prostatectomy: frequency, MRI characteristics, and clinical relevance. AJR Am J Roentgenol 2006;186(2):539–546.

22. Hricak H, Carrington BM. MRI of the pelvis: a text atlas. London, England: Martin Dunitz, 1991.

23. Lassen PM, Kearse WS Jr. Rectal injuries during radical perineal prostatectomy. Urology 1995;45(2):266–269.

24. Yang DM, Jung DH, Kim H, et al. Retroperitoneal cystic masses: CT, clinical, and pathologic findings and literature review. RadioGraphics 2004;24(5):1353–1365.

25. Cirillo S, Petracchini M, Scotti L, et al. Endorectal magnetic resonance imaging at 1.5 Tesla to assess local recurrence following radical prostatectomy using T2-weighted and contrast-enhanced imaging. Eur Radiol 2009;19(3):761–769.

26. Sella T, Schwartz LH, Swindle PW, et al. Suspected local recurrence after radical prostatectomy: endorectal coil MR imaging. Radiology 2004;231(2):379–385.

27. Casciani E, Polettini E, Carmenini E, et al. Endorectal and dynamic contrast-enhanced MRI for detection of local recurrence after radical prostatectomy. AJR Am J Roentgenol 2008;190(5):1187–1192.

28. Sciarra A, Panebianco V, Salciccia S, et al. Role of dynamic contrast-enhanced magnetic resonance (MR) imaging and proton MR spectroscopic imaging in the detection of local recurrence after radical prostatectomy for prostate cancer. Eur Urol 2008;54(3):589–600.

29. Cookson MS, Aus G, Burnett AL, et al. Variation in the definition of biochemical recurrence in patients treated for localized prostate cancer: the American Urological Association Prostate Guidelines for Localized Prostate Cancer Update Panel report and recommendations for a standard in

the reporting of surgical outcomes. J Urol 2007;177(2):540–545.

30. Freedland SJ, Sutter ME, Dorey F, Aronson WJ. Defining the ideal cutpoint for determining PSA recurrence after radical prostatectomy. Prostate-specific antigen. Urology 2003;61(2):365–369.

31. Amling CL, Bergstralh EJ, Blute ML, Slezak JM, Zincke H. Defining prostate specific antigen progression after radical prostatectomy: what is the most appropriate cut point? J Urol 2001;165(4):1146–1151.

32. Partin AW, Oesterling JE. The clinical usefulness of prostate specific antigen: update 1994. J Urol 1994;152(5 Pt 1):1358–1368.

33. Yossepowitch O, Bjartell A, Eastham JA, et al. Positive surgical margins in radical prostatectomy: outlining the problem and its long-term consequences. Eur Urol 2009;55(1):87–99.

34. Vargas HA, Akin O, Hricak H. Residual prostate tissue after radical prostatectomy: acceptable surgical complication or treatment failure? Urology 2010;76(5):1136–1137.

35. Pound CR, Partin AW, Eisenberger MA, Chan DW, Pearson JD, Walsh PC. Natural history of progression after PSA elevation following radical prostatectomy. JAMA 1999;281(17):1591–1597.

36. Nielsen ME, Trock BJ, Walsh PC. Salvage or adjuvant radiation therapy: counseling patients on the benefits. J Natl Compr Cancer Netw 2010;8(2):228–237.

37. Trock BJ, Han M, Freedland SJ, et al. Prostate cancer-specific survival following salvage radiotherapy vs observation in men with biochemical recurrence after radical prostatectomy. JAMA 2008;299(23):2760–2769.

38. Siddiqui SA, Mynderse LA, Zincke H, et al. Treatment of prostate cancer local recurrence after radical retropubic prostatectomy with 17-gauge interstitial transperineal cryoablation: initial experience. Urology 2007;70(1):80–85.

39. Murota-Kawano A, Nakano M, Hongo S, Shoji S, Nagata Y, Uchida T. Salvage high-intensity focused ultrasound for biopsy-confirmed local recurrence of prostate cancer after radical prostatectomy. BJU Int 2010;105(12):1642–1645.

40. Fraass BA. The development of conformal radiation therapy. Med Phys 1995;22(11 Pt 2):1911–1921.

41. Sugimura K, Carrington BM, Quivey JM, Hricak H. Postirradiation changes in the pelvis: assessment with MR imaging. Radiology 1990;175(3):805–813.

42. Coakley FV, Hricak H, Wefer AE, Speight JL, Kurhanewicz J, Roach M. Brachytherapy

for prostate cancer: endorectal MR imaging of local treatment-related changes. Radiology 2001;219(3):817–821.

43. Cellini N, Morganti AG, Mattiucci GC, et al. Analysis of intraprostatic failures in patients treated with hormonal therapy and radiotherapy: implications for conformal therapy planning. Int J Radiat Oncol Biol Phys 2002;53(3):595–599.

44. Pucar D, Hricak H, Shukla-Dave A, et al. Clinically significant prostate cancer local recurrence after radiation therapy occurs at the site of primary tumor: magnetic resonance imaging and step-section pathology evidence. Int J Radiat Oncol Biol Phys 2007;69(1):62–69.

45. Sala E, Eberhardt SC, Akin O, et al. Endorectal MR imaging before salvage prostatectomy: tumor localization and staging. Radiology 2006;238(1):176–183.

46. Pucar D, Shukla-Dave A, Hricak H, et al. Prostate cancer: correlation of MR imaging and MR spectroscopy with pathologic findings after radiation therapy-initial experience. Radiology 2005;236(2):545–553.

47. Westphalen AC, Coakley FV, Roach M 3rd, McCulloch CE, Kurhanewicz J. Locally recurrent prostate cancer after external beam radiation therapy: diagnostic performance of 1.5-T endorectal MR imaging and MR spectroscopic imaging for detection. Radiology 2010;256(2):485–492.

48. Rouvière O, Valette O, Grivolat S, et al. Recurrent prostate cancer after external beam radiotherapy: value of contrast-enhanced dynamic MRI in localizing intraprostatic tumor—correlation with biopsy findings. Urology 2004;63(5):922–927.

49. Haider MA, Chung P, Sweet J, et al. Dynamic contrast-enhanced magnetic resonance imaging for localization of recurrent prostate cancer after external beam radiotherapy. Int J Radiat Oncol Biol Phys 2008;70(2):425–430.

50. Kim CK, Park BK, Lee HM. Prediction of locally recurrent prostate cancer after radiation therapy: incremental value of 3T diffusion-weighted MRI. J Magn Reson Imaging 2009;29(2):391–397.

51. Akin O, Gultekin DH, Vargas HA, et al. Incremental value of diffusion weighted and dynamic contrast enhanced MRI in the detection of locally recurrent prostate cancer after radiation treatment: preliminary results. Eur Radiol 2011;21(9):1970–1978.

52. Cox JD, Gallagher MJ, Hammond EH, Kaplan RS, Schellhammer PF. Consensus statements on radiation therapy of prostate cancer: guidelines for prostate re-biopsy after radiation and for radiation therapy with rising prostate-specific antigen levels after radical prostatectomy. American Society for Therapeutic Radiology and Oncology Consensus Panel. J Clin Oncol 1999;17(4):1155.

53. Sheinbein C, Teh BS, Mai WY, Grant W, Paulino A, Butler EB. Prostate-specific antigen bounce after intensity-modulated radiotherapy for prostate cancer. Urology 2010;76(3):728–733.

54. Kirilova A, Damyanovich A, Crook J, Jezioranski J, Wallace K, Pintilie M. 3D MR-spectroscopic imaging assessment of metabolic activity in the prostate during the PSA "bounce" following 125iodine brachytherapy. Int J Radiat Oncol Biol Phys 2011;79(2):371–378.

55. Roach M 3rd, Hanks G, Thames H Jr, et al. Defining biochemical failure following radiotherapy with or without hormonal therapy in men with clinically localized prostate cancer: recommendations of the RTOG-ASTRO Phoenix Consensus Conference. Int J Radiat Oncol Biol Phys 2006;65(4):965–974.

56. Crook J, Malone S, Perry G, Bahadur Y, Robertson S, Abdolell M. Postradiotherapy prostate biopsies: what do they really mean? Results for 498 patients. Int J Radiat Oncol Biol Phys 2000;48(2):355–367.

57. Sartor CI, Strawderman MH, Lin XH, Kish KE, McLaughlin PW, Sandler HM. Rate of PSA rise predicts metastatic versus local recurrence after definitive radiotherapy. Int J Radiat Oncol Biol Phys 1997;38(5):941–947.

58. Stock RG, Cesaretti JA, Unger P, Stone NN. Distant and local recurrence in patients with biochemical failure after prostate brachytherapy. Brachytherapy 2008;7(3):217–222.

59. Ward JF, Sebo TJ, Blute ML, Zincke H. Salvage surgery for radiorecurrent prostate cancer: contemporary outcomes. J Urol 2005;173(4):1156–1160.

60. Paparel P, Cronin AM, Savage C, Scardino PT, Eastham JA. Oncologic outcome and patterns of recurrence after salvage radical prostatectomy. Eur Urol 2009;55(2):404–410.

61. Bianco FJ Jr, Scardino PT, Stephenson AJ, Diblasio CJ, Fearn PA, Eastham JA. Long-term oncologic results of salvage radical prostatectomy for locally recurrent prostate cancer after radiotherapy. Int J Radiat Oncol Biol Phys 2005;62(2):448–453.

62. Sanderson KM, Penson DF, Cai J, et al. Salvage radical prostatectomy: quality of life outcomes and long-term oncological control of radiorecurrent prostate cancer. J Urol 2006;176(5):2025–2031; discussion 2031–2032.

63. van der Poel HG, Beetsma DB, van Boven H, Horenblas S. Perineal salvage prosta-tectomy for radiation resistant prostate cancer. Eur Urol 2007;51(6):1565–1571; discussion 1572.

64. Boukaram C, Hannoun-Levi JM. Management of prostate cancer recurrence after definitive radiation therapy. Cancer Treat Rev 2010;36(2):91–100.

65. Chin JL, Pautler SE, Mouraviev V, Touma N, Moore K, Downey DB. Results of salvage cryoablation of the prostate after radiation: identifying predictors of treatment failure and complications. J Urol 2001;165 (6 Pt 1):1937–1941; discussion 1941–1942.

66. Izawa JI, Madsen LT, Scott SM, et al. Salvage cryotherapy for recurrent prostate cancer after radiotherapy: variables affecting patient outcome. J Clin Oncol 2002;20(11):2664–2671.

67. Benoit RM, Cohen JK, Miller RJ Jr. Cryosurgery for prostate cancer: new technology and indications. Curr Urol Rep 2000;1(1):41–47.

68. Donnelly BJ, Saliken JC, Ernst DS, et al. Role of transrectal ultrasound guided salvage cryosurgery for recurrent prostate carcinoma after radiotherapy. Prostate Cancer Prostatic Dis 2005;8(3):235–242.

69. Bahn DK, Lee F, Silverman P, et al. Salvage cryosurgery for recurrent prostate cancer after radiation therapy: a seven-year follow-up. Clin Prostate Cancer 2003;2(2):111–114.

70. Eisenberg ML, Shinohara K. Partial salvage cryoablation of the prostate for recurrent prostate cancer after radiotherapy failure. Urology 2008;72(6):1315–1318.

71. Nguyen PL, Chen MH, D'Amico AV, et al. Magnetic resonance image-guided salvage brachytherapy after radiation in select men who initially presented with favorable-risk prostate cancer: a prospective phase 2 study. Cancer 2007;110(7):1485–1492.

72. Tharp M, Hardacre M, Bennett R, Jones WT, Stuhldreher D, Vaught J. Prostate high-dose-rate brachytherapy as salvage treatment of local failure after previous external or permanent seed irradiation for prostate cancer. Brachytherapy 2008;7(3):231–236.

73. Lee HK, Adams MT, Motta J. Salvage prostate brachytherapy for localized prostate cancer failure after external beam radiation therapy. Brachytherapy 2008;7(1):17–21.

74. Murat FJ, Poissonnier L, Rabilloud M, et al. Mid-term results demonstrate salvage high-intensity focused ultrasound (HIFU) as an effective and acceptably morbid salvage treatment option for locally radiorecurrent prostate cancer. Eur Urol 2009;55(3):640–647.

75. Chalasani V, Martinez CH, Lim D, Chin J. Salvage HIFU for recurrent prostate cancer

after radiotherapy. Prostate Cancer Prostatic Dis 2009;12(2):124–129.

76. Ahmed HU, Ishaq A, Zacharakis E, et al. Rectal fistulae after salvage high-intensity focused ultrasound for recurrent prostate cancer after combined brachytherapy and external beam radiotherapy. BJU Int 2009;103(3):321–323.

77. Huggins C, Hodges CV. Studies on prostatic cancer: I. The effect of castration, of estrogen and of androgen injection on serum phosphatases in metastatic carcinoma of the prostate. 1941. J Urol 2002;168(1):9–12.

78. Bolla M, de Reijke TM, Van Tienhoven G, et al. Duration of androgen suppression in the treatment of prostate cancer. N Engl J Med 2009;360(24):2516–2527.

79. Sharifi N, Gulley JL, Dahut WL. Androgen deprivation therapy for prostate cancer. JAMA 2005;294(2):238–244.

80. Mueller-Lisse UG, Vigneron DB, Hricak H, et al. Localized prostate cancer: effect of hormone deprivation therapy measured by using combined three-dimensional 1H MR spectroscopy and MR imaging: clinico-pathologic case-controlled study. Radiology 2001;221(2):380–390.

81. Mueller-Lisse UG, Swanson MG, Vigneron DB, et al. Time-dependent effects of hormone-deprivation therapy on prostate metabolism as detected by combined magnetic resonance imaging and 3D magnetic resonance spectroscopic imaging. Magn Reson Med 2001;46(1):49–57.

82. Chen M, Hricak H, Kalbhen CL, et al. Hormonal ablation of prostatic cancer: effects on prostate morphology, tumor detection, and staging by endorectal coil MR imaging. AJR Am J Roentgenol 1996;166(5):1157–1163.

83. Secaf E, Nuruddin RN, Hricak H, McClure RD, Demas B. MR imaging of the seminal vesicles. AJR Am J Roentgenol 1991;156(5):989–994.

84. D'Amico AV, Halabi S, Tempany C, et al. Tumor volume changes on 1.5 tesla endorectal MRI during neoadjuvant androgen suppression therapy for higher-risk prostate cancer and recurrence in men treated using radiation therapy results of the phase II CALGB 9682 study. Int J Radiat Oncol Biol Phys 2008;71(1):9–15.

85. Calais da Silva FE, Bono AV, Whelan P, et al. Intermittent androgen deprivation for locally advanced and metastatic prostate cancer: results from a randomised phase 3 study of the South European Uroncological Group. Eur Urol 2009;55(6):1269–1277.

86. Nakata S, Miyazawa Y, Sasaki Y, Nakano K, Takahashi H. Prognostic factors for estrogen therapy of relapsed prostate cancer after maximal androgen blockade (MAB)

[in Japanese]. Nippon Hinyokika Gakkai Zasshi 2010;101(4):597–602.

87. Dale W, Hemmerich J, Bylow K, Mohile S, Mullaney M, Stadler WM. Patient anxiety about prostate cancer independently predicts early initiation of androgen deprivation therapy for biochemical cancer recurrence in older men: a prospective cohort study. J Clin Oncol 2009;27(10):1557–1563.

88. Bonney WW, Fallon B, Gerber WL, et al. Cryosurgery in prostatic cancer: survival. Urology 1982;19(1):37–42.

89. Onik GM, Cohen JK, Reyes GD, Rubinsky B, Chang Z, Baust J. Transrectal ultrasound-guided percutaneous radical cryosurgical ablation of the prostate. Cancer 1993;72(4):1291–1299.

90. Marberger M, Carroll PR, Zelefsky MJ, et al. New treatments for localized prostate cancer. Urology 2008;72(6 Suppl):S36–S43.

91. Blana A, Murat FJ, Walter B, et al. First analysis of the long-term results with transrectal HIFU in patients with localised prostate cancer. Eur Urol 2008;53(6):1194–1201.

92. Gelet A, Chapelon JY, Poissonnier L, et al. Local recurrence of prostate cancer after external beam radiotherapy: early experience of salvage therapy using high-intensity focused ultrasonography. Urology 2004; 63(4):625–629.

93. Vogl TJ, Eichler K, Mack MG, et al. Interstitial photodynamic laser therapy in interventional oncology. Eur Radiol 2004;14(6): 1063–1073.

94. Brown SB, Brown EA, Walker I. The present and future role of photodynamic therapy in cancer treatment. Lancet Oncol 2004;5(8):497–508.

95. Pauly KB, Diederich CJ, Rieke V, et al. Magnetic resonance-guided high-intensity ultrasound ablation of the prostate. Top Magn Reson Imaging 2006;17(3):195–207.

96. Siddiqui K, Chopra R, Vedula S, et al. MRI-guided transurethral ultrasound therapy of the prostate gland using real-time thermal mapping: initial studies. Urology 2010;76(6):1506–1511.

97. Kalbhen CL, Hricak H, Shinohara K, et al. Prostate carcinoma: MR imaging findings after cryosurgery. Radiology 1996;198(3): 807–811.

98. Rouvière O, Lyonnet D, Raudrant A, et al. MRI appearance of prostate following transrectal HIFU ablation of localized cancer. Eur Urol 2001;40(3):265–274.

99. Kirkham AP, Emberton M, Hoh IM, Illing RO, Freeman AA, Allen C. MR imaging of prostate after treatment with high-intensity focused ultrasound. Radiology 2008;246(3):833–844.

100. Haider MA, Davidson SR, Kale AV, et al. Prostate gland: MR imaging appearance after vascular targeted photodynamic therapy with palladium-bacteriopheophorbide. Radiology 2007;244(1):196–204.

101. Parivar F, Hricak H, Shinohara K, et al. Detection of locally recurrent prostate cancer after cryosurgery: evaluation by transrectal ultrasound, magnetic resonance imaging, and three-dimensional proton magnetic resonance spectroscopy. Urology 1996;48(4):594–599.

102. Donnelly SE, Donnelly BJ, Saliken JC, Raber EL, Vellet AD. Prostate cancer: gadolinium-enhanced MR imaging at 3 weeks compared with needle biopsy at 6 months after cryoablation. Radiology 2004;232(3):830–833.

103. Kim CK, Park BK, Lee HM, Kim SS, Kim E. MRI techniques for prediction of local tumor progression after high-intensity focused ultrasonic ablation of prostate cancer. AJR Am J Roentgenol 2008;190(5):1180–1186.

104. Rouvière OG, Girouin N, Glas L, et al. Prostate cancer transrectal HIFU ablation: detection of local recurrences using T2-weighted and dynamic contrast-enhanced MRI. Eur Radiol 2010;20(1):48–55.

105. Leibovici D, Zisman A, Lindner A, Stav K, Siegel YI. PSA elevation during prostate cryosurgery and subsequent decline. Urol Oncol 2005;23(1):8–11.

106. Wieder J, Schmidt JD, Casola G, vanSonnenberg E, Stainken BF, Parsons CL. Transrectal ultrasound-guided transperineal cryoablation in the treatment of prostate carcinoma: preliminary results. J Urol 1995;154(2 Pt 1):435–441.

107. Greene GF, Pisters LL, Scott SM, Von Eschenbach AC. Predictive value of prostate specific antigen nadir after salvage cryotherapy. J Urol 1998;160(1):86–90.

108. Ellis DS. Cryosurgery as primary treatment for localized prostate cancer: a community hospital experience. Urology 2002; 60(2 Suppl 1):34–39.

109. Shinohara K, Rhee B, Presti JC Jr, Carroll PR. Cryosurgical ablation of prostate cancer: patterns of cancer recurrence. J Urol 1997; 158(6):2206–2209; discussion 2209–2210.

110. Poissonnier L, Chapelon JY, Rouvière O, et al. Control of prostate cancer by transrectal HIFU in 227 patients. Eur Urol 2007; 51(2):381–387.

111. Bahn DK, Lee F, Badalament R, Kumar A, Greski J, Chernick M. Targeted cryoablation of the prostate: 7-year outcomes in the primary treatment of prostate cancer. Urology 2002;60(2 Suppl 1):3–11.

112. Blana A, Rogenhofer S, Ganzer R, Wild PJ, Wieland WF, Walter B. Morbidity associated with repeated transrectal high-intensity focused ultrasound treatment of localized prostate cancer. World J Urol 2006;24(5): 585–590.